Foam Fractionation

G. Narsimhan, Purdue University, West Lafayette, IN, USA

Introduction

Foam concentration/fractionation is a separation technique in which surface-active solutes are either concentrated from a dilute solution or separated from a mixture by preferential adsorption at a gas–liquid interface created by sparging an inert gas through the solution. These gas bubbles entrain the surfactant solution and form a stable foam with a large gas–liquid interfacial area. As the foam moves through the column, the surfactant solution tends to drain due to gravity and capillary forces. This results in a decrease in the amount of liquid in the foam. The reduction in the entrained liquid is first associated with the bubbles forming the closest spherical packing, after which they will deform to a dodecahedral shape and then possibly coalesce. Consequently, there is an increase in the gas–liquid interfacial area per unit volume of the liquid. The surfactant tends to adsorb preferentially at the gas–liquid interface. At the top of the column, the foam is sent to a foam breaker where the foam is broken either mechanically or chemically. This results in either enrichment or concentration of more surface-active protein because of the recovery of adsorbed protein from the gas–liquid interface into the bulk entrained liquid. In the case of a dilute solution of a single protein, the extent of enrichment would depend upon the relative amount of adsorbed protein compared to that in the bulk entrained liquid. In the case of a mixture of proteins in solution, the separation of a protein from the mixture would depend upon the extent of preferential adsorption of that protein at the gas–liquid interface. Since the adsorption isotherm usually leads to a much higher proportion of adsorbed protein at very low bulk concentrations, foam concentration is very effective for extremely dilute solutions.

Because of the presence of hydrophilic and hydrophobic functional groups, proteins are surface active. Therefore, foam-based separations are viable for concentration/separation of protein solutions. Foam-based separation has been applied to various proteins and enzymes. Experimental investigation has been summarized in **Table 1**. This review highlights the theoretical aspects of prediction of enrichment and separation of proteins and enzymes in a foam fractionation column.

Different Modes of Operation of a Foam Column

Figure 1 depicts the different modes of operation of a foam fractionation column. The simplest mode is the production of a protein-rich concentrate phase from a dilute aqueous protein solution. This can be operated as semi-batch mode (Figure 1A), in which a pool of protein solution is maintained at the bottom

Table 1 Foam fractionation of proteins

Proteins separated	*Experimental set-up*	*Reference*
Choline esterase	Batch	Schultz, 1937; Bader *et al.*, 1944
Pepsin, rennin	Batch	Andrews and Schultz, 1945
Sodium cholate	Batch	Bader *et al.*, 1944
Apple proteins	Semi-batch	Davis *et al.*, 1949
Bovine serum albumin	Batch	Schnepf and Gaden, 1959 Gehle and Schugerl, 1984
Bovine serum albumin	Continuous	Ahmad, 1975a,b Brown *et al.*, 1990 Uraizee and Narsimhan, 1996
Potato proteins	Batch with recycle	Weijenberg *et al.*, 1978
Catalase, amylase	Batch	Charm *et al.*, 1966
Streptokinase	Batch	Holmstrom, 1968
Lysozyme, human serum albumin	Batch	Lalchev and Exerowa, 1981
Acid phosphatase	Batch	London and Hudson, 1953
Urease, catalase	Batch	London *et al.*, 1954
Bovine serum albumin-DNA, lysozyme-DNA	Batch	Lalchev *et al.*, 1982
Placental proteins	Continuous	Sarkar *et al.*, 1987

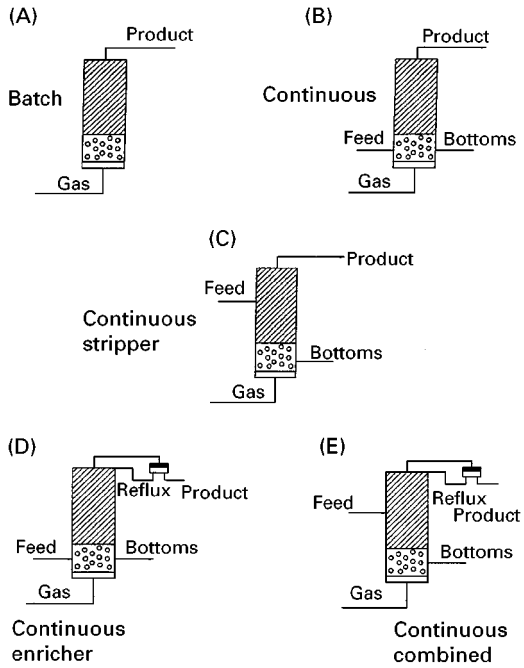

Figure 1 Different modes of operation of a foam fractionation column.

of a column and is sparged with an inert gas which forms the foam. The foam is continuously removed at the top of the column, sent to a foam breaker and the top product collected. Since the most surface-active protein is preferentially removed from the solution, the solution would progressively get depleted in that protein as time progresses. As a result, the pool would get enriched in other components in the case of mixtures. In continuous operation, a feed stream of protein solution is introduced into the pool and the bottom product withdrawn (Figure 1B). Sparging of gas bubbles mixes the liquid pool well enough so that the bottom product is at the same composition as the liquid pool. In addition, the continuous foam column can also be operated in stripping, enriching or combined modes. In the stripping mode, the object is to remove, almost completely, protein from a dilute solution. In this mode, the feed is introduced into the foam and trickles down countercurrently through the rising foam (Figure 1C). The protein concentration in the liquid below the feed-point falls with foam depth, due to it being adsorbed on to the rising bubble surface. There is a net upflow of solution through the foam maintained by entrained up-flowing liquid from the pool. If the foam column is deep enough the protein adsorbed on the bubble surface Γ_F, will be in equilibrium with the feed liquid concentration c_F, and the pool liquid concentration will be very low. Consequently, the bottom product is stripped of more protein than that in the simple mode of operation. In the enriching mode (Figure 1D), the feed stream is introduced into the liquid pool and part of the top product that is obtained by collapsing the foam is refluxed into the column. Protein-rich reflux flows down countercurrently through the foam resulting in further enrichment of protein in the top product. In the combined mode (Figure 1E), the feed is introduced into the foam and the external reflux is used. Part of the column above the feed acts as an enricher, whereas the bottom part of the column acts as a stripper.

It is reasonable to assume that the residence time of the bubbles through the liquid pool is sufficiently large for protein adsorption to reach close to equilibrium so that the surface concentration of protein at the gas–liquid interface can be assumed to be close to the equilibrium value. Also, if bubble coalescence in the foam bed is negligible, the concentration of protein in the interstitial liquid can be expected to be the same as that in the liquid pool. For simple mode of operation of the foam column with a continuous feed stream consisting of a dilute protein solution, the top product concentration c_D, is related to the pool concentration c_B via:

$$c_D = c_B + \frac{6G\Gamma_B}{dD} \qquad [1]$$

where G is the gas flow rate, D is the top product flow rate, d is the bubble size and Γ_B is the equilibrium surface concentration of protein at the gas–liquid interface corresponding to the pool concentration. In the above equation, the first term on the right-hand side is the contribution to the protein concentration from the bulk interstitial liquid before the foam is collapsed and the second term is the contribution from the adsorbed protein at the gas–liquid interface which is recovered into the bulk upon collapse of the foam. A mass balance around the column now gives the following equations for the top product concentration c_D and the bottom product concentration c_B respectively (Lemlich, 1968):

$$c_D = c_F + \frac{6G\Gamma_B}{d}\frac{B}{F(F-B)} \qquad [2]$$

and:

$$c_B = c_F - \frac{6G\Gamma_B}{Fd} \qquad [3]$$

where c_F is the feed concentration, c_B is the pool concentration, F is the feed flow rate, and B is the bottoms flow rate. In the case of binary mixture of

two proteins, the separation efficiency S, defined as the ratio of the two enrichments, is given by:

$$S = \frac{c_{D,2}}{c_{F,2}}\frac{c_{F,1}}{c_{D,1}} = \frac{1 + \dfrac{6G\Gamma_2(c_{B,2})}{dc_{F,2}}\dfrac{B}{F(F-B)}}{1 + \dfrac{6G\Gamma_1(c_{B,1})}{dc_{F,1}}\dfrac{B}{F(F-B)}} \quad [4]$$

where the subscripts 1 and 2 refer to components 1 and 2 and $\Gamma_i\,(c_{B,i})$ is the equilibrium surface concentration of component i corresponding to the bulk concentration $c_{B,i}$. It can easily be seen that the separation ratio is greater than unity if component 2 is more surface active than 1. Also, in the above equation factor 6 arises because the area per unit volume of spherical bubbles of diameter d is $6/d$. If the dodecahedral shape of the bubbles in the foam is to be accounted for, factor 6 is to be replaced with 6.59. For a Langmuir adsorption isotherm, the surface concentration of proteins is related to the bulk concentration via:

$$\Gamma_i = \frac{K_i c_i}{1 + \sum_i K_i a_i c_i}, \quad i = 1, 2 \quad [5]$$

where K_i is the equilibrium constant, c_i is the bulk concentration and a_i is the area occupied by a protein molecule.

In the stripping mode, the feed stream is introduced into the foam (Figure 1C). For a long stripping column, the protein concentration of downflowing interstitial liquid will approach that of entrained liquid in the foam. The two concentrations will approach each other at the feed level. Therefore, the protein concentration of the interstitial liquid at the top can be taken to be the feed concentration. Therefore, mass balance around the foam column yields (Lemlich, 1968):

$$c_D = c_F + \frac{6.59G\Gamma_F}{d(F-B)} \quad [6]$$

and:

$$c_B = c_F - \frac{6.59G\Gamma_F}{Bd} \quad [7]$$

where Γ_F is the equilibrium surface concentration of the protein at the gas–liquid interface corresponding to the feed concentration. Since $\Gamma_F \geq \Gamma_B$, $B \leq F$, comparison of eqns [2] and [3] with eqns [6] and [7] indicates that the stripping mode yields a leaner bottom product and richer top product compared to the simple mode of operation. The separation efficiency for a binary mixture is given by:

$$S = \frac{c_{D,2}}{c_{F,2}}\frac{c_{F,1}}{c_{D,1}} = \frac{1 + \dfrac{6.59G\Gamma_2(c_{F,2})}{dc_{F,2}}\dfrac{1}{(F-B)}}{1 + \dfrac{6.59G\Gamma_1(c_{F,1})}{dc_{F,1}}\dfrac{1}{(F-B)}} \quad [8]$$

Analysis of Foam Column for the Prediction of Liquid Hold-up, Enrichment and Separation Factor

Various phenomena that take place in a foam column are shown schematically in **Figure 2**. Bubbles are formed by the sparger into the liquid pool. Proteins adsorb on to the bubbles during their formation and their passage through the liquid pool. The rate of adsorption of protein depends on the rate of diffusion of protein molecules to the gas–liquid interface as well as on the adsorption activation energy at the bubble surface. The extent of the surface coverage at the gas–liquid interface is dependent on the time of formation of the bubbles and its residence time in the liquid pool (Uraizee and Narsimhan, 1995). The foam bed consists of an assemblage of gas bubbles separated by thin liquid films, creating a large gas–liquid interfacial area. The size distribution of the bubbles depends on the type of sparger employed for bubble formation. A sintered disc with fine pores

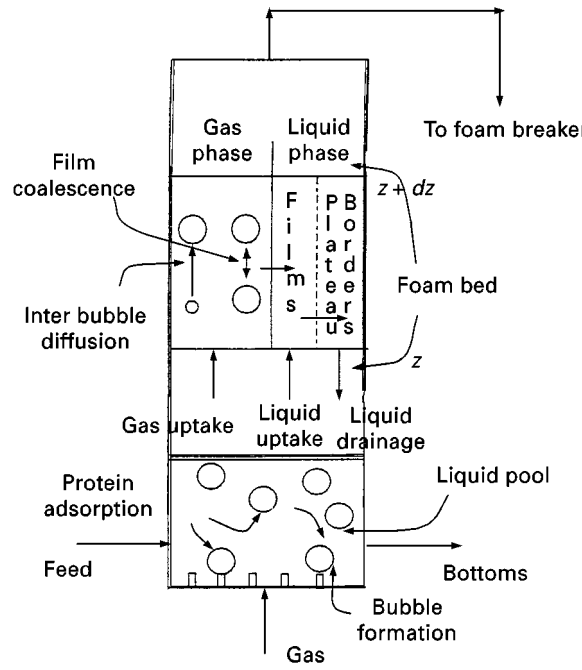

Figure 2 Schematic of various phenomena that take place in a foam column.

usually results in a wide distribution of bubble sizes whereas either capillaries or orifices of uniform sizes lead to more or less uniform bubble sizes. Since the volume fraction of liquid in a foam is usually very small, the gas bubbles are distorted and are usually approximated by a dodecahedron (Narsimhan and Ruckenstein, 1986). A typical gas bubble is shown in **Figure 3A**. The neighbouring gas bubbles are assumed to be separated by planar films of the continuous liquid phase. Where three bubbles touch, their films drain laterally into a Plateau border. This is a channel whose length is the length of a side of the touching dodecahedral bubbles, and whose walls have a sharp concave curvature of radius R_p (Figure 3B). This lateral flow is caused by a pressure drop ΔP between the liquid pressure in the film, which is essentially the air pressure in the bubble, and the pressure of the liquid in the Plateau border. If σ is the surface tension of the bubble–liquid interface, then:

$$\Delta P = \frac{\sigma}{R_p} \qquad [9]$$

The liquid in the Plateau border drains under gravity. Consequently, the liquid hold-up decreases with foam height. The lateral flow out of the thin films separating the gas bubbles will cause them to thin further, possibly causing them to rupture because of instability resulting from the growth of thermal and mechanical perturbations thus leading to bubble coalescence. Coalescence leads to internal reflux of the liquid from the ruptured films into the Plateau borders and a decrease in the interfacial area because of an increase in the bubble size. The former tends to enhance separation (enrichment) whereas the latter is detrimental. The former effect is usually predominant, so that coalescence leads to higher separation (enrichment). Only when coalescence is excessive, collapse of the foam bed occurs. When there is a broad distribution of bubble sizes, diffusion of gas from smaller to larger bubbles may occur because of the difference in the capillary pressure (being inversely proportional to bubble size) thus leading to the growth of larger bubbles at the expense of smaller ones.

In order to predict the liquid hold-up as a function of foam height, one needs to solve the balance equations for drainage of liquid from thin films into the Plateau borders. The equations describing the rate of change, with vertical position, of the volumetric hold-up of the liquid in the films, caused by their drainage into the Plateau borders and bubble coalescence is given by (Uraizee and Narsimhan, 1995):

$$-\frac{\mathrm{d}}{\mathrm{d}z}(\eta n_f A_f x_f) - N n_f A_f V - \frac{N}{2} n_f A_f x_f \beta = 0 \qquad [10]$$

where x_f is the film thickness, n_f is the number of films per bubble, A_f is the area of the film, η is the number of bubbles entrained per unit cross-section of the foam, N is the number of bubbles per unit volume of the foam, and V is the velocity of drainage of the film and β is the coalescence frequency. η and N can be related to the superficial gas velocity G, liquid hold-up ε, and the bubble volume v through:

$$\eta = \frac{G}{v}, \quad N = \frac{1-\varepsilon}{v} \qquad [11]$$

As before, the equation describing the rate of change, with vertical position, of volumetric liquid hold-up in the Plateau borders, caused by flow from the films into the Plateau borders and bubble coalescence, and gravity drainage is given by (Uraizee and Narsimhan, 1995):

$$-\frac{\mathrm{d}}{\mathrm{d}z}(\eta n_p a_p l) + \frac{\mathrm{d}}{\mathrm{d}z}\left(\frac{4}{15} N n_p a_p u R\right) + N n_f A_f V + \frac{N}{2} n_f A_f x_f \beta = 0 \qquad [12]$$

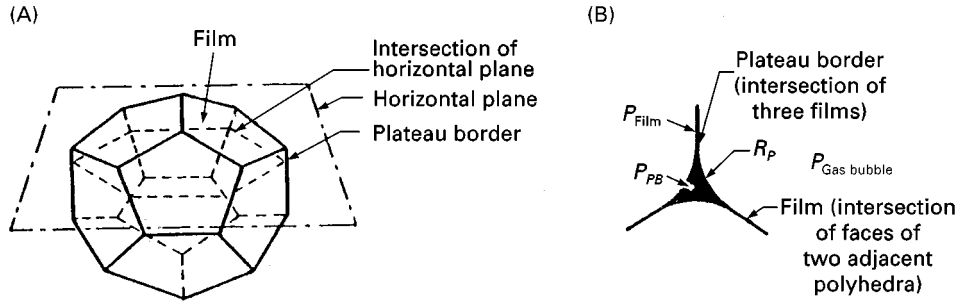

Figure 3 Schematic of a bubble in a foam column.

where n_p is the number of Plateau borders per bubble, a_p is the area of cross-section of Plateau border, R is the radius of the bubble, l is the length of the Plateau border, and u is the velocity of gravity drainage of Plateau borders. Similarly, the protein balance in the foam can be written as:

$$-\frac{\mathrm{d}}{\mathrm{d}z}(\eta n_p a_p l c_{p,i}) + \frac{\mathrm{d}}{\mathrm{d}z}\left(\frac{4}{15} N n_p u R c_{p,i}\right) + N n_f A_f V_f c_{f,i} + \beta \frac{N}{2} n_f A_f x_f c_{f,i} + \beta \frac{N}{2} n_f A_f \Gamma_i = 0, \quad i = 1, 2 \qquad [13]$$

where $c_{p,i}$ and $c_{f,i}$ are the protein concentrations in the Plateau border and film respectively. In the absence of coalescence, they would be equal. However, coalescence would enrich the liquid in the Plateau border because of reflux of adsorbed protein from the ruptured thin films. In the above equation, Γ_i is related to the bulk concentration c_i via the Langmuir adsorption isotherm given by eqn [5]. In eqns [12] and [13], V and u are the velocities of drainage of films and Plateau borders, respectively. For an immobile gas–liquid interface, the velocity of drainage of films into the Plateau borders can be evaluated from the Reynolds equation:

$$V = \frac{2}{3} \frac{\Delta P x_f^3}{\mu R_f^2} \qquad [14]$$

where R_f is the radius of the film, μ is the viscosity, and ΔP is the pressure drop under which the film drains. The velocity of drainage of the Plateau borders for immobile gas–liquid interface is given by:

$$u = \frac{\rho g a_p}{20\sqrt{3}\mu} \qquad [15]$$

where ρ is the density of the liquid.

Eqns [10], [12] and [13] are initial value problems which have to be solved with proper initial conditions at the foam–liquid interface to evaluate x_f and a_p and $c_{p,i}$ as a function of foam height.

The liquid hold-up at the foam–liquid interface ($z = 0$) can be set to the void fraction of spheres (Uraizee and Narsimhan, 1995):

$$\varepsilon_0 = N n_f A_f x_{f0} + N n_p a_{p0} l = 0.26 \qquad [16]$$

As the liquid hold-up at the top of the column is much smaller than 0.26, the flow rate at the top of the column is much smaller than the entrainment of the liquid at the foam–liquid interface. Hence, the material balance around the foam yields:

$$\frac{G\varepsilon_0}{1-\varepsilon_0} = \frac{4}{15} N_0 n_p a_{p0} u R_0 \qquad [17]$$

The inlet bubble size R_0 depends on the type of sparger and the superficial gas velocity G. The above two equations can be solved for x_{f0} and a_{p0}. Also, the protein concentration in films and Plateau borders at the foam–liquid interface can be taken as equal to the pool concentration, i.e.:

$$c_{f0} = c_{p0} = c_B \qquad [18]$$

The pool concentration should satisfy the overall protein balance given by:

$$F c_F = B c_B + T c_T \qquad [19]$$

where F, B and T refer to feed, bottom and top product flow rates expressed per unit area of cross-section of the foam column. The overall mass balance can be written as:

$$F = B + T \qquad [20]$$

Eqns [10] to [13] can be solved with the initial conditions [16] to [20] to give the profiles of x_f, a_p and $c_{p,i}$. The liquid hold-up ε at any foam height can then be calculated via:

$$\varepsilon = N n_f A_f x_f + N n_p a_p l \qquad [21]$$

The enrichment e_i for each component is given by (Uraizee and Narsimhan, 1995):

$$e_i = \frac{(N n_f A_f x_f c_{f,i} + N n_p a_p l c_{p,i} + N n_f A_f \Gamma_i)_T}{c_{F,i}\varepsilon_T} \qquad [22]$$

where $(\ldots)_T$ refers to the evaluation of the quantity within the parenthesis at the top of the column. The separation factor S is then given by:

$$S = \frac{e_2}{e_1} \qquad [23]$$

The above analysis assumes adsorption equilibrium for the surface concentration of proteins at the

air–water interface. Uraizee and Narsimhan (1995) have modified this analysis to account for the kinetics of adsorption of proteins on to the gas bubbles during their travel through the liquid pool before the formation of foam and demonstrated the effects of different parameters including the kinetics of adsorption and pool height on enrichment and recovery of proteins.

Effect of Operating Conditions on Enrichment and Separation

The operating conditions that can be varied in a foam column are the superficial gas velocity G, the bubble size R, the column height L, feed flow rate F, the feed concentration c_f and the mode of operation. In addition, the separation will also be influenced by the viscosity of the feed and the extent of bubble coalescence in the foam column.

Protein enrichment depends on the total amount of protein selectively adsorbed at the gas–liquid interface as well as on the liquid hold-up in the foam. Smaller liquid hold-ups result in a larger interfacial area per unit volume of the liquid and therefore in larger enrichment. At higher superficial gas velocities, more liquid is entrained by the gas bubbles from the liquid pool leading to higher liquid hold-ups in the foam column and consequently to smaller enrichment. As the bubble size increases, a larger proportion of the liquid that is entrained by the foam is distributed in the film, resulting in a faster drainage rate. On the other hand, an increase in the bubble size results in a decrease in the interfacial area per unit volume. Because of the above two opposing effects, there exists an optimum bubble size at which enrichment may be maximum (Narsimhan and Ruckenstein, 1986) for one component protein solution as shown in **Figure 4**. In addition, this maximum is found to be more pronounced at smaller superficial gas velocities. Narsimhan and Ruckenstein (1986) have developed a population balance model to account for the bubble size distribution in the description of drainage and coalescence in a foam bed. Their model was able to predict the change in the bubble size distribution as a result of coalescence. The results indicated collapse of the foam bed for broader inlet bubble size distribution with a coefficient of variation above a critical value. In the case of a mixture of proteins, however, the separation efficiency would depend on the preferential adsorption of one protein over the other components as can be seen from eqns [22] and [23]. As expected, the separation efficiency is higher for the protein which adsorbs the most at the gas–liquid interface with a higher value of Γ. As a result, the separation efficiency

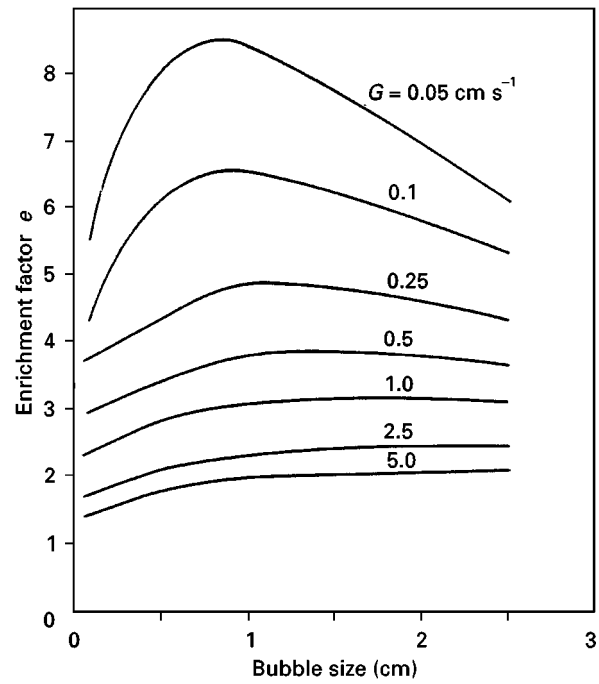

Figure 4 Effect of the inlet bubble size on the enrichment for $\mu = 10^{-2}$ P, $\mu_s = 10^{-4}$ sP, and $c_0 = 10^{-7}$ gmol mL^{-1}. (Reproduced with permission from Narsimhan and Ruckenstein, 1986a.)

would be higher for larger values of Langmuir adsorption parameter K_i as can be seen from eqn [5]. An increase in the viscosity of the feed would result both in a larger amount of liquid entrained by the foam as well as slower liquid drainage leading to larger liquid hold-up. Also, an increase in the viscosity of the feed would tend to stabilize the foam resulting in lower bubble coalescence. Both these effects will result in lower protein enrichment. Bubble coalescence in a foam column leads to: (i) an increase in the protein concentration due to internal reflux with subsequent increase in the surface concentration; (ii) a decrease in the liquid hold-up because of increased liquid drainage rates as a result of larger bubble sizes; and (iii) a decrease in the total surface area because of larger bubble sizes. The first effect results in more protein adsorption per unit area at the gas–liquid interface. The second effect leads to higher surface area per unit volume of the liquid. The third effect leads to a decrease in the total amount of protein adsorbed at the interface. Consequently, the first two effects lead to an increase in the enrichment and separation whereas the second and third effects lead to lower recovery. The second effect may be predominant since coalescence was found to result in an increase in protein enrichment as well as recovery (Uraizee and Narsimhan, 1995). The separation efficiency, as one would expect, depends on the relative

surface activities of proteins in a binary mixture. For larger values of Langmuir isotherm constant K_i (more surface active), the separation efficiency increases. In fact, the calculations show that the separation efficiency increases linearly with the ratio K_2/K_1 (Uraizee and Narsimhan, 1997). However, the separation efficiency was found to decrease rapidly with the feed concentration of the protein (Uraizee and Narsimhan, 1997).

Brown *et al.* (1990) measured enrichment and recovery in a continuous foam concentration column for bovine serum albumin (BSA). In their experiments, foam was generated by sparging nitrogen gas through a glass frit. As a result, the foam consisted of nonuniform size distribution of bubbles. They compared the experimental data with predictions based on a model similar to the one described above but neglecting drop coalescence. Their experimental data showed a decrease in the protein enrichment with superficial gas velocity. The model predictions agreed fairly well for the highest feed concentration of 0.1 wt% as shown in **Figure 5**. The experimental enrichments were found to be larger than the model predictions (even for the largest bubble size in the foam) with the deviation being larger at lower feed concentrations. This was believed to be due to the fact that drop coalescence in the foam column became increasingly important at lower feed concentrations as confirmed by experimental measurements of bubble size with the height of the column.

Uraizee and Narsimhan (1996) also observed a decrease in enrichment with gas velocity for foam concentration of BSA in their continuous foam concentration experiments in which the foam was generated by sparging nitrogen through a capillary bundle thus resulting in a foam of uniform bubble sizes. In their experiments, the residence time of the bubbles in the liquid pool was varied by varying the pool height. Interestingly, protein enrichment was found to increase with pool height at sufficiently high pool heights, thus indicating the importance of kinetics of adsorption of protein on to the gas–liquid interface on enrichment. At low pool heights, however, they observed an increase in protein enrichment with a decrease in pool height due to excessive bubble coalescence in the foam. Their model, which accounted both for the kinetics of protein adsorption as well as coalescence, was able to explain the increase in protein enrichment due to bubble coalescence at small pool heights and an increase in enrichment with pool heights at larger pool heights. A comparison of the experimental data with their model predictions is shown in **Figure 6**.

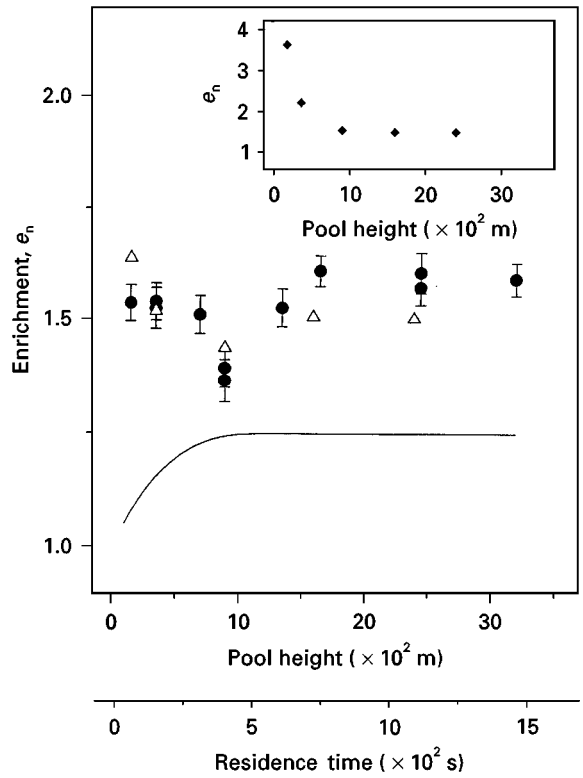

Figure 6 Comparison of experimental results with model predictions for BSA; feed concentration 0.1 wt%, bubble diameter 1.9×10^{-3} m, gas velocity 2.6×10^{-3} m s^{-1}, foam height 1.3×10^{-1} m, $F = 2 \times 10^{-5}$ m s^{-1}, pH 4.8, ionic strength 0.1 M. (●) Experimental data. (△) Model predictions accounting for kinetics of adsorption as well as coalescence. (—) Model predictions accounting only for kinetics of adsorption. (◆) Model prediction accounting only for coalescence assuming equilibrium surface concentration is shown in the inset. (Reproduced with permission from Uraizee and Narsimhan (1996).)

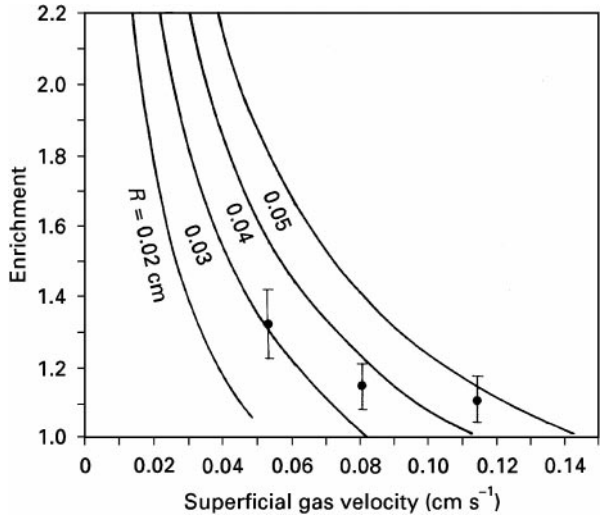

Figure 5 Effect of superficial gas velocity on protein enrichment for $c_F = 0.1$ wt%. $F = 0.02$ cm s^{-1}, $I = 0.1$ M, pH = 7, $z = 5$ cm. The curves refer to model predictions for different bubble sizes. (Reproduced with permission from Brown *et al.*, 1990.)

Ahmed (1975) observed an increase in the separation efficiency of albumin with the superficial gas velocity with the value reaching a plateau at sufficiently high gas velocities. Schnepf and Gaden (1959) and Ahmad (1975) reported a maximum protein enrichment at the isoelectric point of the protein which can be explained by the maximum protein adsorption at the interface due to the absence of electrostatic energy barrier for adsorption. However, this maximum was found to be considerably less pronounced at higher protein concentrations. Protein enrichment was also influenced by the change in the bubble size at different pH (Brown *et al.*, 1990). Separation efficiency of albumin was found to decrease dramatically as the foam height increased from 3 to 17 cm (Ahmed, 1975). Even though enrichment increased with foam height because of internal reflux resulting from increased drop coalescence, the top product flow rate was also found to decrease dramatically due to faster drainage. As a result, the protein separation was less at higher foam heights. Ahmed (1975) also found that the introduction of the feed stream into the foam instead of liquid pool increased the separation efficiency because the foam column was operated in the combined mode with an enricher and stripper.

In conclusion, the main attractive features of foam fractionation are its low capital and operating costs. Therefore, it can be employed as a first step for preconcentration/separation before more expensive separation methods can be used. More work is needed to establish the applicability of foam fractionation as a viable separation method for mixtures of proteins and to develop new processes based on this technique. Few experimental data are available on the adsorption isotherm and kinetics on to gas–liquid interface for mixtures of proteins. More importantly, it is necessary to probe denaturation (if any) of proteins and enzymes when subjected to foaming.

See also: **II/Flotation:** Bubble-Particle Capture; Froth Processes and the Design of Column Flotation Cells; Historical Development.

Further Reading

Ahmed SI (1975) Laws of foam formation and foam fractionation. 1. The effect of different operating parameters on the foam fractionation of albumin from a solution containing organic and inorganic materials. *Separation Science* 10: 673.

Ahmed SI (1975) Laws of foam formation and foam fractionation. 2. The influence of different association conditions on surfactants, glycerides, sugar and salts on the foam fractionation of albumins. *Separation Science* 10: 689.

Bader R, Schultz F and Stacey M (1944) A crystalline serum mucoprotein with high choline esterase activity. *Nature* 154: 183.

Bader R and Schultz F (1946) Fractionation by adsorption and crystallization on foam. Part II. Experiments with bile salts. *Transactions of the Faraday Society* 42: 571.

Brown LK, Narsimhan G and Wankat PC (1990) Foam fractionation of globular proteins. *Biotechnology and Bioengineering* 36: 947.

Charm SE, Morningstar J, Matteo C and Paltiel B (1966) The separation and purification of enzymes through foaming. *Analytical Biochemistry* 15: 498.

Davis SG, Fellers CR and Esselen WB (1949) Application of foam fractionation procedures to the isolation of fruit juices. *Food Technology* 3: 198.

Gehle RD and Schugerl K (1984) Protein recovery by continuous fractionation. *Applied Microbiology Biotechnology* 20: 133.

Holmstrom B (1968) Foam concentration of streptokinase from crude culture filtrates. *Biotechnology and Bioengineering* 10: 551.

Lalchev Z, Dimitrova L, Txvetkova P and Exerowa D (1982) Foam separation of DNA and proteins from solutions. *Biotechnology and Bioengineering* 24: 2253.

Lalchev A and Exerowa D (1981) Concentration of proteins by foaming. *Biotechnology and Bioengineering* 23: 669.

Lemlich R (1968) Principles of foam fractionation. In: Perry ES (ed.) *Progress in Separation and Purification*, vol. 1, pp. 1–56. New York: Interscience.

London M, Cohen M and Hudson P (1954) Some general characteristics of enzyme foam fractionation. *Biochimica Biophysica Acta* 13: 111.

London M and Hudson P (1953) Studies on the purification of acid prostatic phosphatase. *Archives of Biochimica Biophysica Acta* 46: 141.

Narsimhan G and Ruckenstein E (1986) Hydrodynamics, enrichment and collapse in foams. *Langmuir* 2: 230.

Narsimhan G and Ruckenstein E (1986) Effect of bubble size distribution on the enrichment and collapse in foams. *Langmuir* 2: 494.

Sarkar P, Bhattacharya P, Mukherjee RN and Muckerjee M (1987) Isolation and purification of protease from human placenta by foam fractionation. *Biotechnology and Bioengineering* 29: 934.

Schnepf RW and Gaden EL (1959) Foam fractionation of proteins: Concentration of aqueous solutions of BSA. *Journal of Biochemical, Microbiological and Technological Engineering* 1: 1.

Schultz F (1937) Adsorption on foams. *Nature* 139: 629.

Uraizee F and Narsimhan G (1995) A model for continuous foam concentration of proteins: Effects of kinetics of adsorption of proteins and coalescence of foam. *Separation Science and Technology* 36(6): 847.

Uraizee F and Narsimhan G (1996) Effects of kinetics of adsorption and coalescence on continuous foam concentration of proteins: Comparison of experimental results with model predictions. *Biotechnology and Bioengineering* 51: 384.

Weijenberg DC, Mulder JJ, Drinkenburg AAH and Stemerding S (1978) The recovery of protein from potato juice waste water by foam separation. *Journal of Engineering and Chemical Processing, Design and Development* 17: 209.

Froth Processes and the Design of Column Flotation Cells

I. M. Flint, Canadian Process Technologies Inc., Vancouver, BC, Canada
M. A. Burstein, NPACI Edcenter on Computational Science and Engineering, San Diego State University, San Diego, CA, USA

Introduction

The function of a flotation column is selectively to separate certain suspended solid particles or liquid droplets based on their surface properties. Bubbles rise and particles (drops) settle within the vessel, and collisions are highly dependent on gravitational momentum. The vessel is a multiphase contacting/heterocoagulation device where the dispersed phase to be removed attaches to the bubbles and accumulates at the top of the column in the form of froth. The latter overflows to launders. In this quiescent system, transport, dispersion and mixing of materials are induced by the motion of gas bubbles in the continuous liquid medium.

For the purpose of designing columns, immiscible liquid droplets are considered as acting as solid spheres of an appropriate size and density: thus, a 'particle' may represent either a solid or a liquid.

Almost all flotation columns are operated in the countercurrent regime where slurry moves downwards against a continuous rising bubble swarm. This type of flow increases efficiency (selectivity) of separation as the distance between discharge ports for overflow and underflow is large. In some cases, for example for the flotation of very coarse particles, co-current columns can be considered in order to increase particle residence time and reduce loaded bubble rise time. Unless otherwise stated, all of this article is related to countercurrent columns.

Initial Design Data

The feed transport fluid must be characterized in terms of liquid flow rate and chemical composition. Component solids or immiscible liquid flow rate, material composition and size distribution must also be known. In all cases, mean values, standard deviations and design maxima and minima are required.

Test work must be done, or approximations made, to determine the flotation characteristics of the material to be separated, including rate constants and maximum recovery for all material and particle (droplet) size fractions. Process targets must be well understood, including the desired quality of products and recovery. Data error must be minimized since it directly impacts on the accuracy of the design scale-up.

Site-specific information is also required for final designs. This includes limitations in dimensions due to plant layout, civil engineering specifications, including such items as wind loading, earthquake considerations, supporting platforms and others.

General Dimensions

Typically, columns range in height from 6 to 15 m. This height is dictated by the dimensions of the different zones within the column but is most influenced by the collection zone height.

Column cross-sections are usually round or rectangular. Cylindrical columns do not have special flow conditions at the corners. They, therefore, usually have a more uniform air and feed distribution, less tank weight due to the self-supporting nature of the structure and less wall area per unit operating volume. Rectangular columns use floor space more efficiently and are easier to baffle. The cross-sectional area is usually constant throughout the vessel and is determined by carrying capacity and residence time considerations in the collection and froth zones. Typical industrial cell cross-sectional areas range from less than 1 m^2 to more than 12 m^2.

Column Zones

The flotation column, as generally built, is composed of a number of distinct zones. Under the spargers there is a dead volume (underflow zone) which is only used to remove slurry from the vessel. The volume between the spargers and the feed port is called the collection zone. The volume between the feed port